SLAC-PUB-1270
(T/E)
July 1973

FORWARD NEUTRINO SCATTERING AS A TEST OF PCAC *

Roscoe Giles†
Stanford Linear Accelerator Center
Stanford University, Stanford, California 94305

ABSTRACT

The cross-section for $\nu + N \rightarrow \mu$ + anything is given by PCAC when the muon emerges in the forward direction and its mass is neglected. We estimate corrections to this result due to the muon mass and for slightly non-forward scattering. The PCAC contribution is sizable only over a restricted region of muon transverse momentum and inelasticity. We discuss the implications of these restrictions for experiments designed to test PCAC in this process and give numerical results. We find that modifications to pion dominated PCAC such as those recently proposed by Drell are observable, but counting rates are low and separation of such effects from other corrections may be ambiguous.

(Submitted to Phys. Rev.)

---

*Work supported in part by the U.S. Atomic Energy Commission.
†Fellow of Fannie and John Hertz foundation.

I. INTRODUCTION

Recently, several schemes that modify the simple assumption of pion pole dominance in applications of PCAC have been proposed.[1,2] These schemes are primarily designed to give suitable corrections to low energy applications of PCAC, such as $\pi^0 \to 2\gamma$. However, as originally observed by Adler,[3] there is also a high energy test of PCAC in inelastic neutrino scattering, $\nu + N \to \ell +$anything, where the matrix element for lepton (ℓ) emerging in the forward direction is dominated by the divergence of the axial current. The proposed modifications to pion pole dominated PCAC predict significant deviations of the Adler cross section from the naive PCAC result.

In this paper, we discuss some practical aspects of the use of the Adler experiment as a test of PCAC. The problem is that the dominance of the cross section by the divergence of the axial current is exact only for zero mass leptons emerging exactly in the forward direction. In practice, because the only high flux neutrino beams consist of muon neutrinos, the lepton mass is of the same order of magnitude as the pion mass. Further, any realistic measurement of the cross section relies on a detector with finite angular acceptance, so that one must consider deviations from the PCAC prediction for scattering in slightly nonforward directions. We estimate these nonforward and lepton mass corrections to the modified PCAC prediction for forward neutrino-nucleon scattering. This estimate indicates that PCAC contributions are sizable compared to these corrections only for a restricted kinematic region of inelasticity and lepton transverse momentum. We discuss the experimental implications of these constraints, and estimate the counting rate for a simple, idealized experiment using the full high energy neutrino flux from a beam modelled after that anticipated at NAL.

II. CALCULATION OF CROSS SECTION

We use 4-vectors as defined in Fig. 1. In the lab: $p = (M, 0, 0, 0)$, $k = (E, 0, 0, E)$, $k' = (E', \underline{\Delta}, xE)$ with $E' = \sqrt{\mu^2 + \Delta^2 + x^2E^2}$, where Δ is a small transverse momentum, x is the elasticity, and E, xE are assumed to be large. Let μ = muon mass, W = mass of hadronic state produced, $\nu = E - E'$. To lowest order in μ^2, Δ^2, $-q^2 = \mu^2\left(\frac{1}{x} - 1\right) + \frac{\Delta^2}{x}$.

We use Drell's[1] notations and results for contributions to PCAC from higher mass states, approximated as a particle π' with large mass $m_{\pi'} >> m_\pi$. Neutrino and antineutrino scattering are treated together with most of the necessary subscripts suppressed. Strangeness changing weak currents will be neglected altogether.

The squared, spin averaged matrix element is

$$P = 2G^2\, t^{\mu\nu} M_{\mu\nu} \quad ,$$

where

$$t^{\mu\nu} = k^\mu k'^\nu + k^\nu k'^\mu - k \cdot k'\, g^{\mu\nu} \pm \epsilon^{\mu\nu\lambda\sigma}\, k_\lambda\, k'_\sigma$$

$$M_{\mu\nu} = \frac{1}{2} \sum_s \sum_n \langle ps | J^+_\mu(0) | n \rangle \langle n | J_\nu(0) | ps \rangle\, (2\pi)^4\, \delta^4(p_n - p - q)$$

$\pm$ refer to $\nu, \bar{\nu}$ scattering respectively and J is the appropriate weak current. With the approximation $\mu^2 = \Delta^2 = 0$, k, k , and q are collinear with $q = (1-x)k$. Then $t^{\mu\nu} = \left[2x/(1-x)^2\right] q^\mu q^\nu$ and we obtain the PCAC result. To extract this piece, write

$$P = 2G^2 \left[\frac{2x}{(1-x)^2} P_0 + P_{corr}\right]$$

$$P_0 = q^\mu q^\nu\, M_{\mu\nu} = \text{PCAC contribution}$$

and

$$P_{corr} = \left[t^{\mu\nu} - \frac{2x}{(1-x)^2} q^\mu q^\nu \right] M_{\mu\nu}$$

Using CVC and PCAC modified by the π' contribution:

$$P_0 = \frac{1}{2} \sum_{spin} \sum_{n} \left| \sqrt{2}\, f_\pi C_\pi T_{\pi N \to n} + \sqrt{2}\, f_{\pi'} T_{\pi' N \to n} \right|^2$$

$$\times (2\pi)^4 \, \delta^4 (p_n - p - q)$$

where f_π, $f_{\pi'}$ are the π, π' decay constants. To lowest order

$$C_\pi = \frac{m_\pi^2}{m_\pi^2 - q^2} \approx \frac{x}{\left(\frac{\mu^2 + \Delta^2}{m_\pi^2} \right) + \left(1 - \frac{\mu^2}{m_\pi^2} \right) x}$$

and

$$C_{\pi'} = \frac{m_{\pi'}^2}{m_{\pi'}^2 - q^2} \approx 1 \qquad \text{since} \qquad m_{\pi'}^2 >> -q^2 \ .$$

Following Drell,[1] we can estimate the π' contribution in the resonance and in the high energy regions:

$$f_{\pi'} T_{\pi' N \to n} \approx -.1\, f_\pi T_{\pi N \to n} \qquad \text{for} \qquad W < W_{res} \approx 2.5 \text{ GeV} \ .$$

At high energy, we neglect π-π' interference so that we can write

$$P_0 = 2 f_\pi^2 P_{\pi N \to \text{anything}} \times \begin{cases} (.9)^2 C_\pi^2 & W < W_{res} \\ C_\pi^2 + R_0 & W >> W_{res} \end{cases}$$

with

$$R_0 \equiv \frac{f_{\pi'}^2 \, \sigma^{tot}_{\pi' N} (\nu \to \infty)}{f_\pi^2 \, \sigma^{tot}_{\pi N} (\nu \to \infty)} \ .$$

One has very little handle on the intermediate region where $\pi\pi'$ interference may be important. We assume that the proportionality exhibited at high energy persists down to $W = W_{res}$. This assumption is made only for the purpose of facilitating estimates of the π' contribution. The actual behavior of the cross section for small W is a potential object of experimental investigation.

Drell estimates $R_0 \sim \frac{1}{2}$. Preparata,[2] whose approach is quite different, obtains an equivalent formula for the high energy behavior of P_0 with $R_0 \sim 1$. The practical question is whether R_0 is measurable in the Adler experiments.

Using

$$\sigma_{\pi N} = \frac{P_{\pi N}}{4M\, q_{\pi,\,\mathrm{lab}}} \quad ,$$

we have:

$$P_0 = 8M\, q_{lab}\, f_\pi^2\, \sigma_{\pi N} \left[C_\pi^2 + R(W)\right] \quad ,$$

$$q_{lab} = \text{lab momentum of a pion of energy } \nu \ .$$

$$R(W) = \begin{cases} -.19\, C_\pi^2 & W < W_{res} \\ R_0 & W > W_{res} \end{cases}$$

We estimate the lepton mass and transverse momentum corrections to lowest order in μ^2 and Δ^2. The hadronic tensor $M_{\mu\nu}$ can be written in terms of 5 structure functions that are free of kinematic singularities:

$$M_{\mu\nu} = -G_1(\nu, q^2)\, g_{\mu\nu} + G_2(\nu, q^2) \frac{p_\mu p_\nu}{M^2}$$

$$+ i \frac{G_3(\nu, q^2)}{2M^2}\, \epsilon_{\mu\nu\lambda\sigma}\, q^\lambda p^\sigma + G_4(\nu, q^2) \frac{q_\mu q_\nu}{M^2} + G_5(\nu, q^2) \frac{q_\mu p_\nu + q_\nu p_\mu}{M^2} \ .$$

We can decompose the G_i in terms of vector and axial contributions:

$$G_i = G_i^{VV} + G_i^{AA} \quad \text{for } i \neq 3$$
$$G_3 = G_3^{VA}, \quad \text{an interference term}$$

After some algebra, one finds

$$P_c = \left[\frac{1-4x+x^2}{x(1-x)^2}\Delta^2 + \frac{1-3x}{x(1-x)}\mu^2\right] G_1(\nu, q^2)$$
$$+ \frac{1+3x}{2x(1-x)}(\mu^2+\Delta^2)\, G_2(\nu, q^2) \mp \frac{\nu}{2M}\left[\frac{1+x}{x(1-x)}\Delta^2 + \frac{\mu^2}{x}\right] G_3(\nu, q^2)$$
$$+ \frac{1}{M^2}\left[-2k\cdot k'(k\cdot k'-\mu^2) - \frac{2x}{(1-x)^2}q^4 - q^2(k\cdot k')\right] G_4(\nu, q^2)$$
$$+ \frac{2\nu}{M}\left[\frac{2}{(1-x)^2}\Delta^2 + \frac{1}{1-x}\mu^2\right] G_5(\nu, q^2) \quad . \tag{1}$$

where each kinematic coefficient is written to leading order in μ^2/M^2, Δ^2/M^2.

For a lowest order expansion we need only consider $G_i(\nu, q^2=0)$. At $q^2=0$, the VV structure functions, except G_4, are expressible in terms of the isovector photoabsorption cross section

$$G_1^{VV} = \frac{\nu}{M} G_5^{VV} = \frac{2M\nu}{\pi\alpha}\sigma_{\gamma N}^{I=1}$$

$$G_2^{VV} = 0 \quad .$$

G_2^{AA} can be expressed using PCAC. $G_2^{AA}(\nu, 0) = P_0/\nu$, with P_0 as calculated above.

G_1^{AA} and G_5^{AA} are not yet experimentally accessible. For simplicity and convenience, we assume exact chirality for these form factors, taking $G_1^{AA} = G_1^{VV}$ and $G_5^{AA} = G_5^{VV}$. Using positivity of $M_{\mu\nu}$, we can parametrize G_3 as $\nu/2M\ G_3(\nu, 0) = \rho_3(\nu)\, G_1(\nu, 0)$ where $|\rho_3| \leq 1$. The quantities $(1 \pm \rho_3)G_1$ are the amplitudes for absorption of ± 1 helicity chiral photons on the nucleon.

The G_2 and G_4 terms in (1) can be neglected. The coefficient of G_4 is of order $\Delta^4, \Delta^2\mu^2, \mu^4$ so we drop this term for a lowest order expansion. The G_1 and G_5 terms depend on x as $\nu/M(1-x)^2 = E/M(1-x)$, while the G_2 term goes as $M/\nu(1-x) = M/E(1-x)^2$. The ratio of these factors is $E^2(1-x)/M$. For inelastic scattering $(1-x)_{min} \sim m_\pi/E$. So the ratio of the G_1 term to the G_2 term $\sim Em_\pi/M^2$, which is large at high energy. That the G_2 term is small is simply a check that all the leading PCAC contributions are contained in P_0.

Putting in the above expressions for G_i, one finds

$$P_c^{\pm} = \frac{4M\nu}{\pi\alpha}\,\sigma_{\gamma N}^{I=1}\,\frac{1}{x(1-x)^2}\left\{\left(1+x^2 \mp (1-x^2)\,\rho_3\right)\Delta^2 + (1-x)^2\,(1\mp\rho_3)\,\mu^2\right\}$$

The cross section is

$$S(x,\Delta^2,E) \equiv \frac{d\sigma}{dx\,d\Delta^2}$$

$$= \frac{G^2}{2\pi^2}\,\frac{1}{1-x}\left\{\frac{q_{lab}}{\nu}\,f_\pi^2\,(C_\pi^2+R)\,\sigma_{\pi N}\right.$$

$$\left. + \frac{\sigma_{\gamma N}^{I=1}}{4\pi\alpha}\,\frac{1}{x^2}\left[\left(1+x^2 \mp (1-x^2)\,\rho_3\right)\Delta^2 + (1-x)^2\,(1\mp\rho_3)\,\mu^2\right]\right\}$$

$$= S_\pi + S_{\pi'} + S_c \qquad (2)$$

III. DISCUSSION AND NUMERICAL CALCULATIONS

The qualitative features of S are evident from (2): $S(x,\Delta^2,E)$ depends on E only the resonance region, 1-x small, where $\sigma_{\gamma N}$, $\sigma_{\pi N}$ are not yet asymptotic. All contributions to S grow like $\frac{1}{1-x}$ as $x \to 1$. The correction terms grow rapidly as $x \to 0$ (except when $\rho_3 = \pm 1$) due to the rapid increase in $|q^2|$. Further, for small x or large Δ^2, the pole extrapolation factor C_π^2 suppresses

S_π relative to $S_{\pi'}$ and S_c. $S_{\pi'}$ has no such suppression factor as long as $|q^2| \ll m^2_{\pi'}$.

In order to calculate the relative size of S_c, one must estimate the quantities $\sigma^{I=1}_{\gamma N}$ and ρ_3. From the usual ideas of vector dominance, one believes that real photoabsorption is largely isovector in character so that taking $\sigma_{\gamma N}(I=1) \approx \sigma_{\gamma N}$(real photon) is certainly a reasonable approximation here. ρ_3 is very inaccessible experimentally and theoretically in the region of large ν and small q^2. Fortunately, our qualitative conclusions will be insensitive to ρ_3, except for small x where S_c is markedly reduced for $\rho_3 \rightarrow \pm 1$. As a representative value, we take $\rho_3=0$ for most of the following calculations. S_π, $S_{\pi'}$ and S_c are computed for νp scattering at E = 50 GeV. The results for $\bar{\nu}p$ scattering are qualitatively the same, and, as remarked above, S is independent of E above resonance. We use $R_0 = \frac{1}{2}$ to obtain $S_{\pi'}$.

The resulting values of S are plotted in Figs. 2 and 3. Figures 2a-2d show S plotted against x in the region above resonances for Δ=0, 100, 200, and 300 MeV. Figures 3a and 3b show S vs Δ at x=.5 and .8. We see that $S_{\pi'}$ is quite large compared to S_π and represents a significant deviation from the pure pion pole evaluation of PCAC. However, in much of the x-Δ plane, S_c is also large. Figure 4 shows the region in x-Δ for which $S_c \lesssim \frac{1}{2} S_{tot}$, and indicates that one can hope to see $S_{\pi'}$ over S_c only at moderate inelasticities, $x \gtrsim .4$, and small transverse momenta $\Delta \lesssim 250$ MeV. Outside of this region, S_c is as large or larger than $S_{\pi'}$.

Figure 5 shows S_c vs x at Δ=100 MeV for several values of ρ_3. For $-1 \leq \rho_3 \leq .5$ and $x \geq .4$ S_c varies by less than a factor 1.4 above or below $S_c(x, \rho_3=0)$, which does not really modify the qualitative discussion above. The

significant decrease in S_c for $\rho_3 = 1$ as $x \to 0$ occurs because the lowest order μ correction to $t^{\mu\nu}$ projects out only the helicity -1 part of the amplitude. If $\rho_3 > .5$, prospects for measuring $S_{\pi'}$ can only be improved.

IV. EXPERIMENTAL ASPECTS

In principle, one could measure $d\sigma/d\Delta^2$ in the region of minimal S_c described above and do an optimal fit to Eq. (2), thus obtaining $S_{\pi'}$ and R_0. There are two basic experimental problems that make such a direct approach impracticable. First, the multiple scattering of outgoing muons in a large target-detector apparatus would typically be expected to be on the order 100 - 150 MeV, making transverse momentum resolution poor below 250 MeV. Second, the cross section is very small — at present and anticipated neutrino fluxes, the counting rates into small cells of x-Δ phase space would be much to low to allow a determination of $d\sigma/dxd\Delta^2$. Further, no high flux monochromatic neutrino beams exist. Thus, in a realistic experiment, E can only be reconstructed, event by event, from calorimetric measurements on the hadronic final state. The accuracy of such calorimetry is highly dependent on the experimental details.

Here, we will consider a simpler experiment that gives some indication of the event rates one might expect under optimum conditions. We look at the k' distribution of muons scattered out of an incident neutrino beam of known spectrum $\rho(E)$. This spectrum is modelled after that anticipated at NAL for neutrinos coming from the high energy (K decay) tail of the full neutrino spectrum. This spectrum may be approximated by the form:

$$\rho(E) \equiv \text{number of neutrinos/cm}^2\text{/GeV/incident proton}$$

$$\sim \rho_0 \, e^{-\lambda(E-E_0)} \qquad \text{for} \quad E \geq E_0 \quad .$$

Values used for ρ_0, λ, and E_0 are given in Table I and correspond, approximately, to those estimated for NAL at 200 and 500 GeV.[4]

The quantity we measure will be

$$F(k', \Delta^2) \equiv d(\text{events})/dk'd\Delta^2 \text{ incident proton}$$

$$= \int_{E_{min}} \frac{dE}{E} \rho(E)\, S\left(x = \frac{k'}{E},\ \Delta^2,\ E\right) \quad .$$

F has contributions from the resonance resonance region, $W_{min} \leq W_{res} = 2.5$ GeV and from the region above resonance. Let F_π^{res}, F_c^{res} be the π and correction terms from the resonance region; and, F_π, $F_{\pi'}$, F_c the π, π' and correction terms above resonance. We are interested in the relative size of $F_{\pi'}$.

These various components have been calculated for νp scattering with $R_0 = 1/2$, $\rho_3 = 0$, taking $W_{min} = M + m_\pi$. F is plotted vs k' at $\Delta = 100$ MeV in Figs. 6a and 6b for the 200 and 500 GeV beam spectra. Because $S(x, \Delta^2, E)$ is only weakly dependent on E, all components of F behave like $e^{-\lambda k'}$ as k' increases. Thus, the ratios F_i/F_{tot} are independent of k' for the various components i. The ratios are given in Table II for $\Delta = 100$ MeV and $\Delta = 200$ MeV.

The uninteresting contributions from the resonance region are large ($\sim 50\%$). An observed muon is quite likely to have been produced nearly elastically by a neutrino of only slightly larger energy. This is an obvious consequence of the form of the spectrum and of the peaking of S(x) for $x \to 1$. If we cannot select for $W \gtrsim 2.5$ GeV, the π' effect is reduced to $\sim 25\%$. Let us suppose that we can do calorimetry on the hadronic final state at least well enough to establish $W_{min} \sim 2.5$ GeV.[5]

Then $F_{\pi'}$ contributes a more respectable 50% to the total rate.

Most of F comes from large x scattering. Typically, the minimum x that is important is $x_{min} \sim [k'/(k'+1/\lambda)]_{min} \sim .6$. In addition to enhancing the

contribution of the resonance region, this effect minimizes the importance of the small x region, where S_c is large and has the greatest dependence on the ρ_3 parameter.

We note that increasing the beam energy from 200 to 500 GeV does little to improve the relative size of $F_{\pi'}$. Except for the weighting of the fixed width of the resonance region and except for overall normalization, F "scales" to a function of $\lambda(k'-E_0)$ alone.

Figures 7a and 7b show the Δ dependence of F. As before, F_c dominates the rate for $\Delta \gtrsim 250$ MeV.

In order to get some idea of the counting rate, consider the following (optimistic) experimental situation, patterned after NAL proposal 1A.[5]

(1) Assume a 90 ton lead target containing $\sim 5.4 \times 10^{31}$ nucleons

(2) Assume the proton beam can deliver 2×10^4 pulses/day with 1.5×10^{13} protons/pulse.

Then the counting rate is

$$N = 1.6 \times 10^{49} \times \int F \, dk' d\Delta^2 \quad .$$

The numerical values of the total rate into $k' > E_0$ and $\Delta \lesssim 250$ MeV are given in Table III. The rate increases dramatically with increasing proton energy. $F \propto \rho_0/\lambda$. As the beam energy increases, ρ_0 increases while λ decreases. The resonance region contributes roughly 50% to the total rate. If we can experimentally reject events with $W \lesssim 2.5$ GeV, these calculations show that the observed rate will be 54% π', 27% corrections, and 19% π.

The counting rates shown in Table III, though small, are certainly workable, particularly at higher beam energies (> 200 GeV). The problem is that, presently, one is not up to these energies nor within a factor of 10 of the indicated flux. In this sense, the above rates are quite optimistic, but, hopefully realistic for the not too distant future.

V. CONCLUSIONS

One should not underestimate the delicacy of the calculations above and the conclusions that follow from them. Because we have so few variable experimental parameters, a "measurement" of R_0 depends critically on the estimate of the correction term. For example, in the experiment discussed above, an event rate twice the π-PCAC prediction reflects corrections, while four times PCAC reflects a π' term with $R_0 \sim 1/2$. If the estimate of corrections is too far off, the experiment, at best, gives only a qualitative indication of the presence or absence of the π' term. The estimate we have made of the corrections is relatively crude. The assumptions and approximations involved were as follows:

(1) Strangeness changing processes were neglected.

(2) Corrections were expanded to lowest order in μ^2, Δ^2. It is to be expected that the next order corrections are down by Δ^2/M^2, $\mu^2/M^2 \sim .065$. This, in itself, is a relatively small error.

(3) G^{VV} was estimated by $\sigma_{\gamma N}$(real photon) and "chirality" was assumed so that $G^{AA} \sim G^{VV}$(+PCAC). The approximation of $\sigma_{\gamma N}^{I=1}$ by $\sigma_{\gamma N}$(real photon) is probably very good. But the assumption $G^{AA} = G^{VV}$ has much less foundation. These approximations were chosen on the basis of simplicity, plausibility, and the absence of experimental data on these quantities.

From detailed measurements of inelastic neutrino scattering in nonforward directions one will get information on the structure functions for large $-q^2$. Hopefully, such information can be used to make more intelligent guesses as to what happens at $q^2=0$.

(4) Perhaps the biggest unknown is the VA interference parameter ρ_3. Again, it is measurable in inelastic neutrino scattering for $-q^2 \gg m_\pi^2$.

(5) One should also keep in mind that the π' itself is an approximate representation of the continuum above the π in the 0^- channel.[1] We have a simple understanding of its properties only at very high energy where π-π' interference vanishes as they both couple to the Pomeron giving the ratio R_0, and at low energy where π' matrix elements can be expressed in terms of corrections to PCAC results like the Goldberger-Treiman relation. In particular, there is an uncertainty of the simple R_0 parameterization in the region just above resonance where π-π' interference may not yet be negligible. Thus, once corrections have been subtracted out, the structure for small W may be richer than has been indicated in this treatment.

The Adler experiment, though difficult, will be do-able in the near future if neutrino fluxes as high as have been predicted can be produced. Despite the difficulties of its analysis, the insights it can give into PCAC are considerable.

Acknowledgements

I would like to thank Sidney Drell for suggesting this investigation and for many useful discussions. I also thank David Ritson and Stanley Brodsky for their helpful advice and discussions.

REFERENCES

1. S. D. Drell, Phys. Rev. D7, 2190 (1973).
2. G. Preparata, Trieste Lectures (1973).
3. S. L. Adler, Phys. Rev. 135B, 963 (1964).
4. R. A. Burnstein, NAL Summer Study SS-180 (1970).
5. D. Cline *et al.*, NAL Proposal 1A.

TABLE I

BEAM SPECTRAL PARAMETERS

Beam	E_0, GeV	λ, GeV^{-1}	ρ_0*
200 GeV	36	.055	6.86
500 GeV	50	.026	17.9

*ρ_0 is in units of 10^{-11} neutrinos/GeV/cm^2/incident proton

TABLE II

FRACTIONAL DECOMPOSITION OF F

		Resonance			Above Resonance			
Beam	Δ, MeV	π	Correction	Total	π	π'	Correction	Total
200 GeV	100	.51	.09	.60	.15	.22	.03	.40
	200	.14	.42	.56	.04	.25	.15	.44
500 GeV	100	.43	.08	.51	.19	.26	.04	.49
	200	.12	.35	.47	.05	.31	.17	.53

TABLE III

RATES

(events/day)

	Resonance			Above Resonance				
	π	Correction	Total	π	π'	Correction	Total	Total
200 GeV Beam								
Rate	3.37	3.40	6.77	.98	2.75	1.35	5.08	11.85
Fraction of total	.284	.287	.571	.083	.232	.114	.429	1.00
Above resonance	--	--	--	.193	.541	.266	1.00	--
500 GeV Beam								
Rate	19.1	19.0	38.1	7.5	21.9	11.6	41.0	79.1
Fraction of total	.241	.240	.481	.095	.227	.147	.519	1.00
Above resonance	--	--	--	.183	.534	.283	1.00	--

FIGURE CAPTIONS

1. Kinematics of $\nu + N \rightarrow \mu + n$.
2. Dependence of S on x for various Δ.
3. Dependence of S on Δ at x = .5 and x = .8.
4. Region in x-Δ where $S_c \leq S_\pi + S_{\pi'}$.
5. Dependence of S_c on x for various ρ_3 at Δ = 100 MeV.
6. Dependence of F on k' for 200 and 500 GeV beams.
7. Dependence of F on Δ.

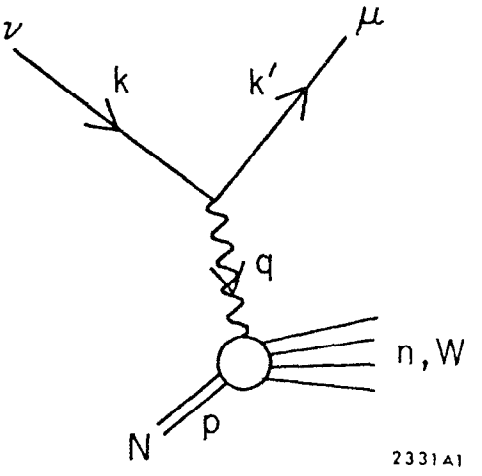

FIG. 1

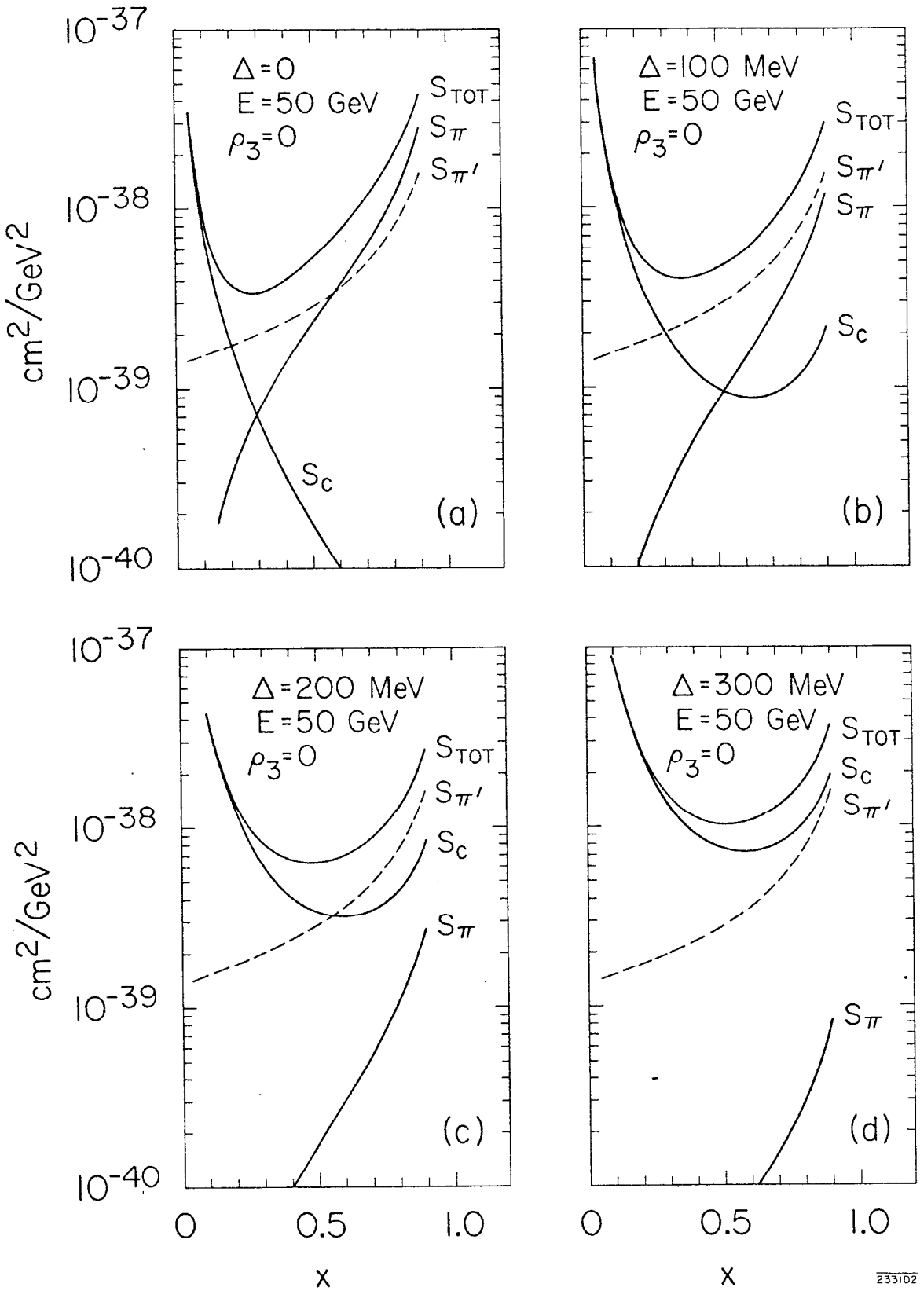
Δ=0
E=50 GeV
ρ3=0
STOT
Sπ
Sπ'
Sc
(a)
Δ=100 MeV
E=50 GeV
ρ3=0
STOT
Sπ'
Sπ
Sc
(b)
Δ=200 MeV
E=50 GeV
ρ3=0
STOT
Sπ'
Sc
Sπ
(c)
Δ=300 MeV
E=50 GeV
ρ3=0
STOT
Sc
Sπ'
Sπ
(d)
cm2/GeV2
10-37
10-38
10-39
10-40
0
0.5
1.0
x
233102

FIG. 2

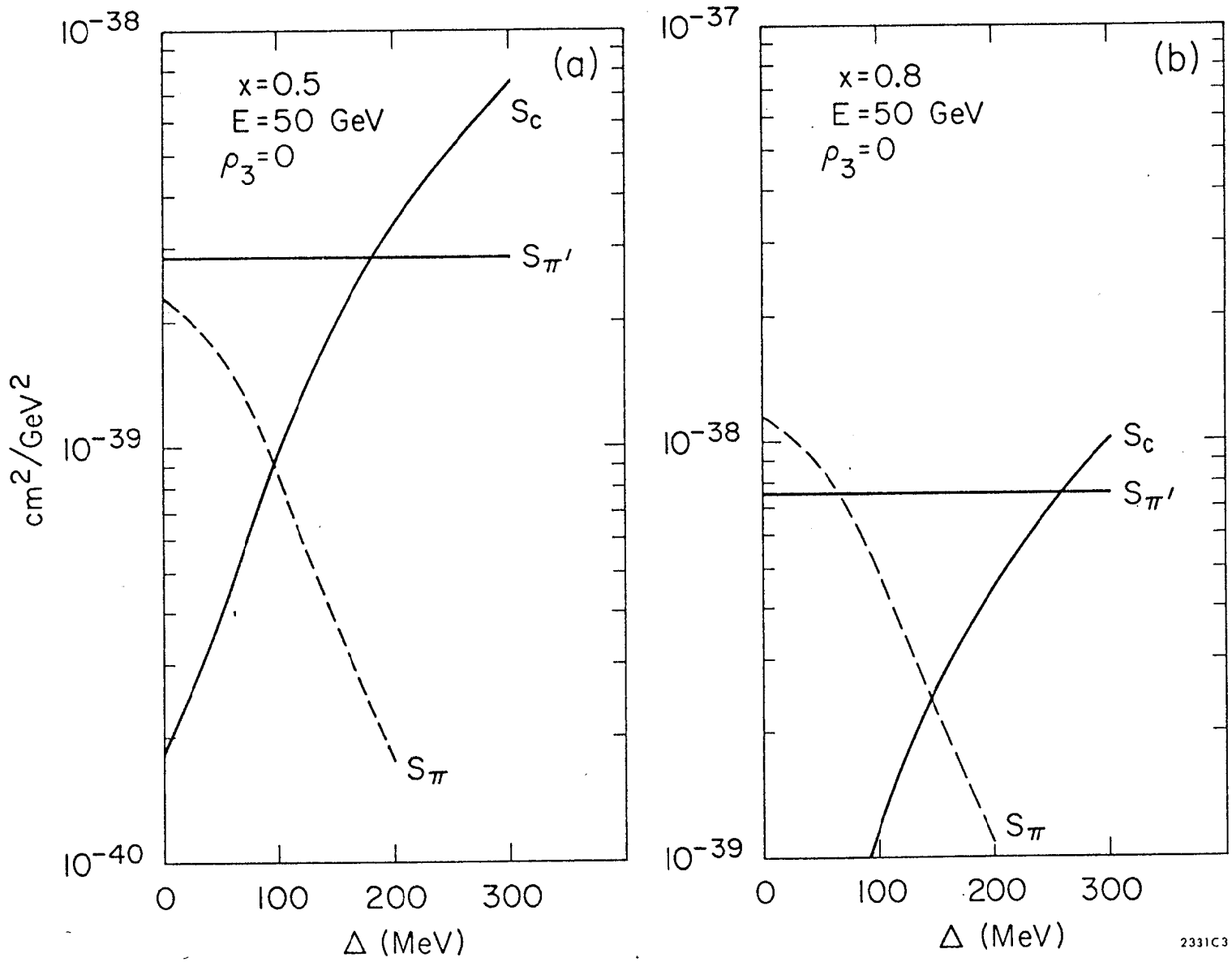
(a)
x=0.5
E=50 GeV
ρ_3=0
S_c
$S_{\pi'}$
S_π
10^{-38}
10^{-39}
10^{-40}
cm^2/GeV^2
0
100
200
300
Δ (MeV)
(b)
x=0.8
E=50 GeV
ρ_3=0
S_c
$S_{\pi'}$
S_π
10^{-37}
10^{-38}
10^{-39}
0
100
200
300
Δ (MeV)
2331C3

FIG. 3

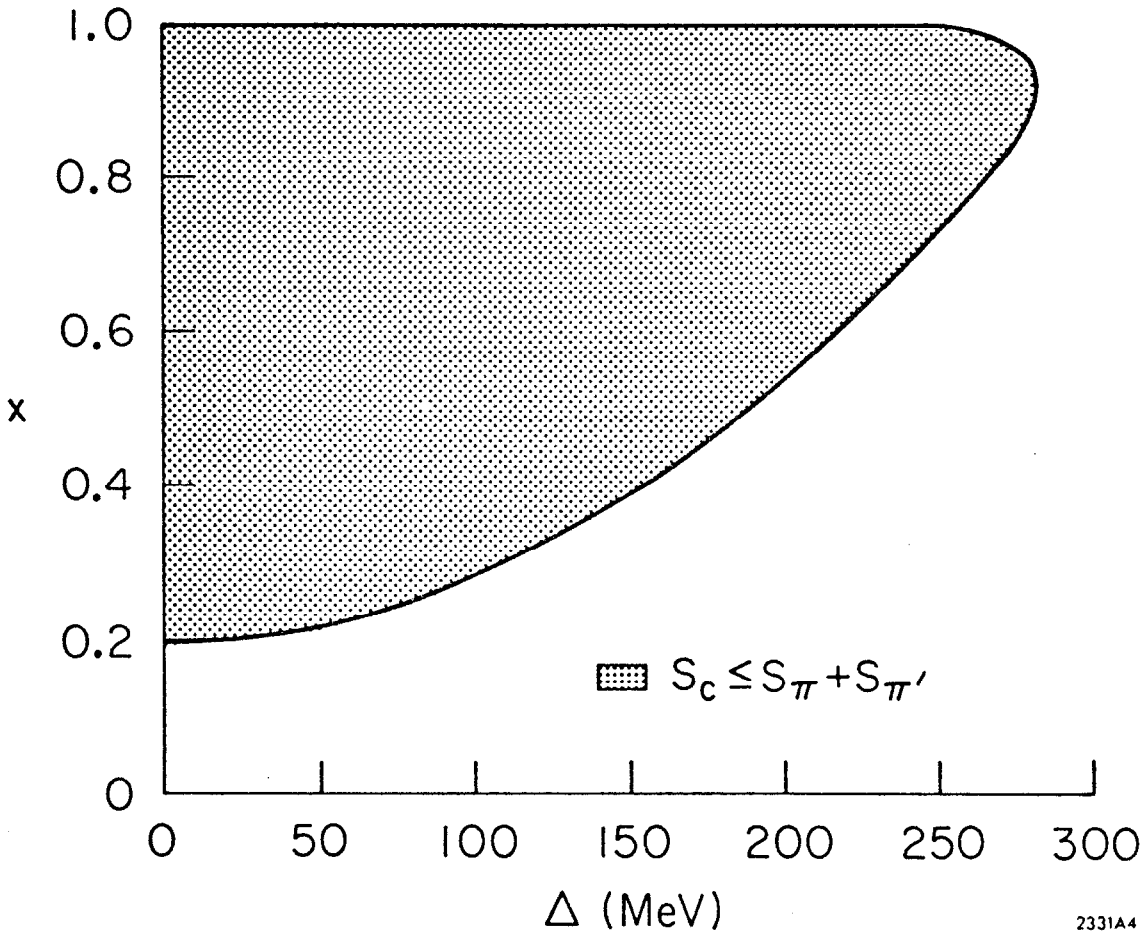
1.0
0.8
0.6
x
0.4
0.2
0
0
50
100
150
200
250
300
Δ (MeV)
$S_c \leq S_\pi + S_{\pi'}$
2331A4

FIG. 4

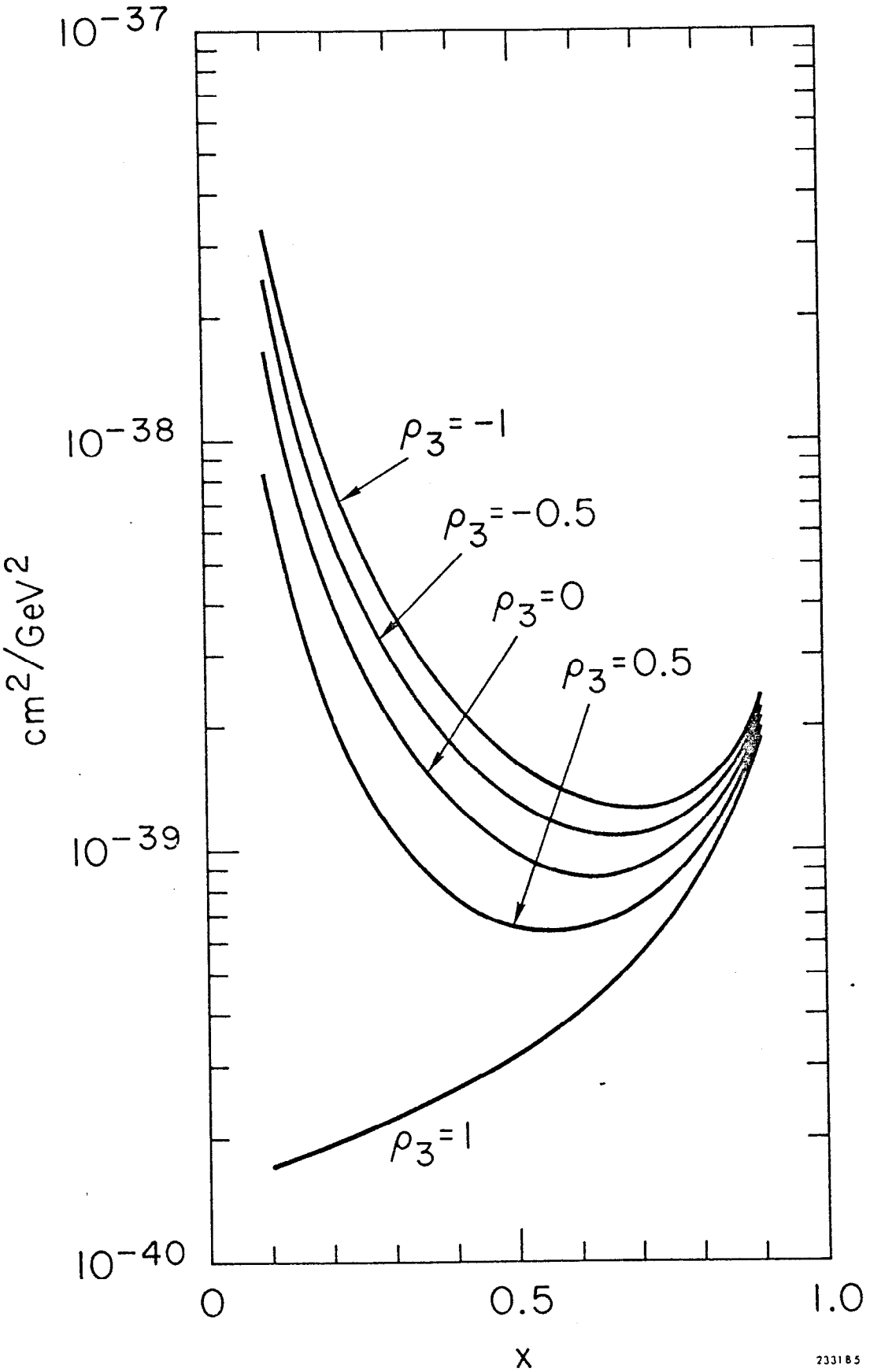
10^{-37}
10^{-38}
10^{-39}
10^{-40}
cm^2/GeV^2
$\rho_3 = -1$
$\rho_3 = -0.5$
$\rho_3 = 0$
$\rho_3 = 0.5$
$\rho_3 = 1$
0
0.5
1.0
x
233185

FIG. 5

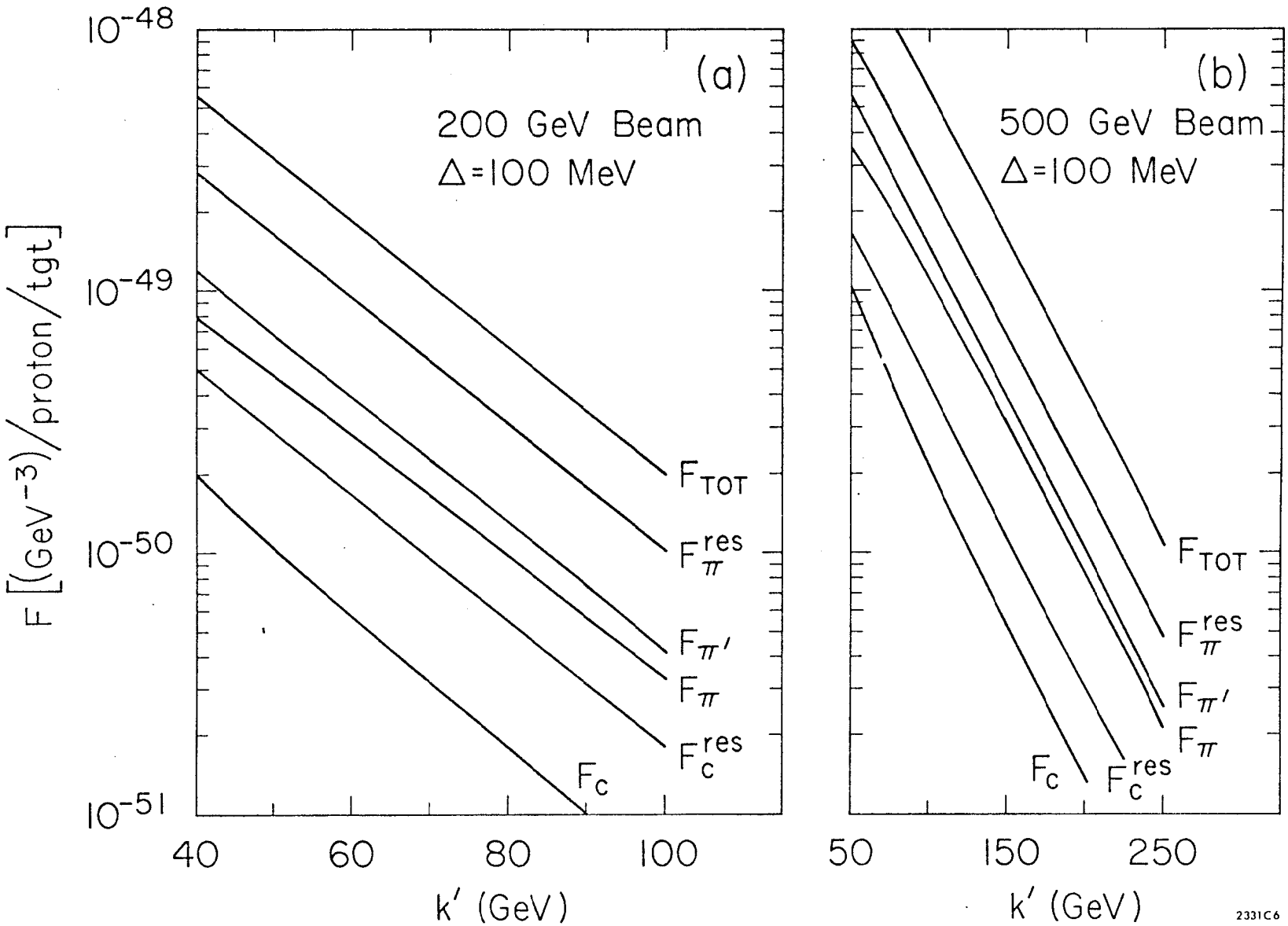
(a)
200 GeV Beam
Δ=100 MeV
(b)
500 GeV Beam
Δ=100 MeV
F [(GeV⁻³)/proton/tgt]
10⁻⁴⁸
10⁻⁴⁹
10⁻⁵⁰
10⁻⁵¹
40
60
80
100
50
150
250
k′ (GeV)
k′ (GeV)
F_TOT
F_π^res
F_π′
F_π
F_c^res
F_c
2331C6

FIG. 6

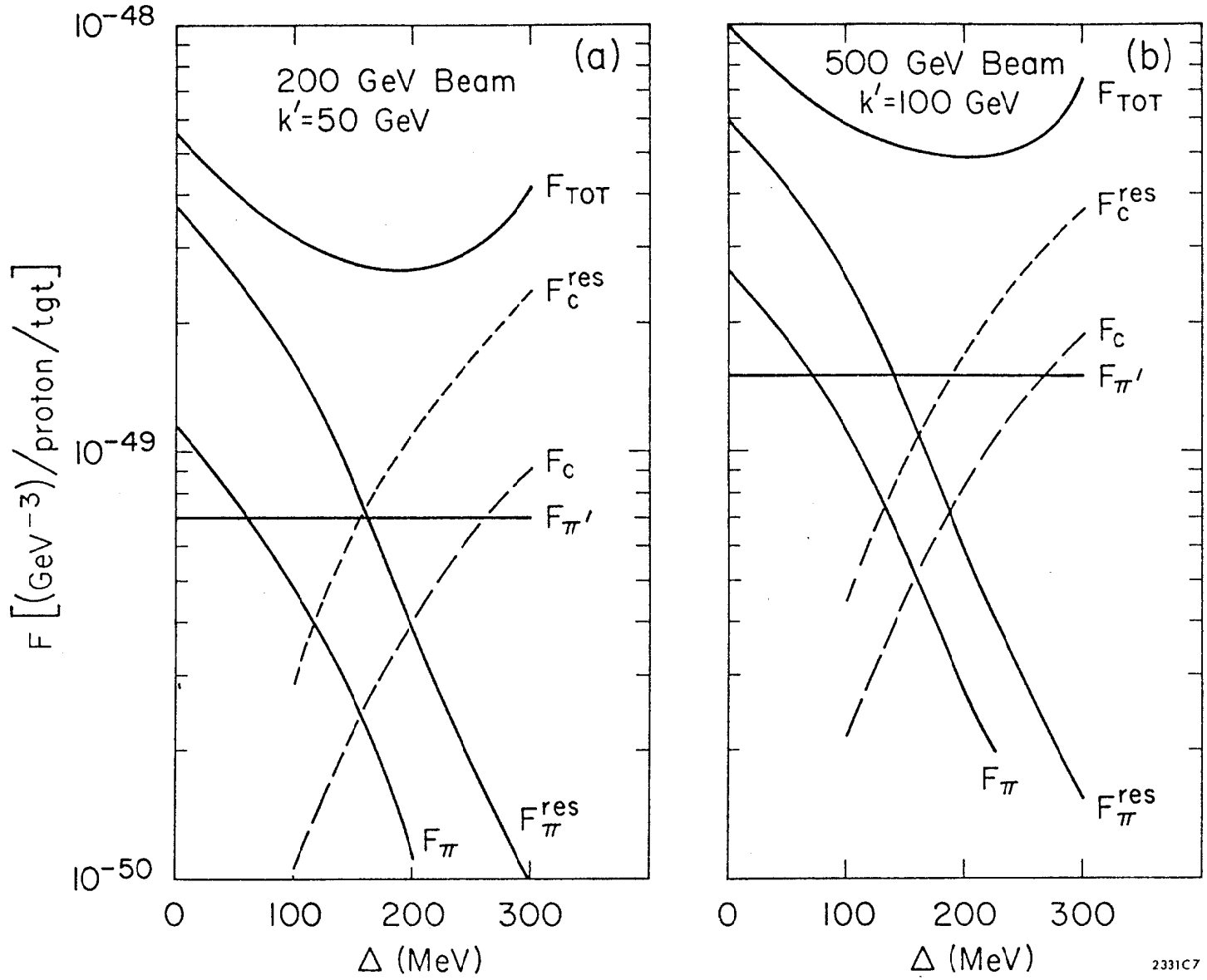
10^-48
10^-49
10^-50
F [(GeV^-3)/proton/tgt]
200 GeV Beam
k'=50 GeV
(a)
F_TOT
F_c^res
F_c
F_π'
F_π
F_π^res
0
100
200
300
Δ (MeV)
500 GeV Beam
k'=100 GeV
(b)
F_TOT
F_c^res
F_c
F_π'
F_π
F_π^res
0
100
200
300
Δ (MeV)
2331C7

FIG. 7